Chemico-Biological Interactions xxx (2015) xxx–xxx

Contents lists available at ScienceDirect

Chemico-Biological Interactions

journal homepage: www.elsevier.com/locate/chembioint

In vitro and *in vivo* evaluation of novel cinnamyl sulfonamide hydroxamate derivative against colon adenocarcinoma

Neetinkumar D. Reddy [a], M.H. Shoja [a], B.S. Jayashree [b], Pawan G. Nayak [a], Nitesh Kumar [a], V. Ganga Prasad [a], K. Sreedhara R. Pai [a], C. Mallikarjuna Rao [a,*]

[a] Department of Pharmacology, Manipal College of Pharmaceutical Sciences, Manipal University, Manipal 576104, Karnataka, India
[b] Department of Pharmaceutical Chemistry, Manipal College of Pharmaceutical Sciences, Manipal University, Manipal 576104, Karnataka, India

ARTICLE INFO

Article history:
Received 26 August 2014
Received in revised form 3 February 2015
Accepted 18 March 2015
Available online xxxx

Keywords:
Colon cancer
Cinnamic acid
HDAC
Apoptosis
Caspase 3/7
1,2-Dimethyl hydrazine (DMH)

ABSTRACT

The potential of cinnamic acid as an anti-inflammatory and anti-cancer agent has been studied previously. In our investigation, novel bio-isosters of cinnamyl sulfonamide hydroxamate were synthesized, characterized and confirmed for their structure and evaluated for cytotoxicity. Three NCEs namely, NMJ-1, -2 and -3 showed cell-growth inhibition in 6 human cancer cell lines with IC_{50} at the range of 3.3 ± 0.15–44.9 ± 2.6 μM. The hydroxamate derivatives of cinnamyl sulfonamide are reported inhibitors of HDAC enzyme. Thus, the effectiveness of these molecules was determined by whole cell HDAC assay in HCT 116 cell line. NMJ-2 (0.41 ± 0.01 μM) exhibited better enzyme inhibition (IC_{50}) compared to SAHA (2.63 ± 0.07). In order to evaluate induction of apoptosis by treatment, Hoechst 33342 and AO/EB nuclear staining methods were used. Further, cell cycle analysis, Annexin V binding and caspase 3/7 activation assays were performed by flow cytometry where NMJ-2 significantly arrested the cell cycle at G_2/M phase, increased Annexin V binding to the cell surface and activation of caspase-3/7. Bax/Bcl-2 ratio was observed by Western blot and showed an increase with NMJ-2 treatment. This was comparable to standard SAHA. The acute toxicity study (OECD-425) showed that NMJ-2 was safe up to 2000 mg/kg in rats. 1,2-Dimethyl hydrazine (DMH) was used to produce experimental colon adenocarcinoma in Wistar rats. 5-FU and NMJ-2 (100 mg/kg *p.o.* and 10 mg/kg *i.p.* once daily for 21 days, respectively) were administered to the respective groups. Both treatments significantly reduced ACFs, adenocarcinoma count, TNF-α, IL-6, nitrite and nitrate levels in colonic tissue. Our findings indicate that NMJ-2 has potent anti-cancer activity against colon cancer, by acting through HDAC enzyme inhibition and activation of intrinsic mitochondrial apoptotic pathway, with additional anti-inflammatory activity.

1. Introduction

Cancer has reached epidemic proportions globally and accounts for 12 million cases worldwide and 7.9 million deaths [1]. It accounts for 13% of all deaths each year with the most common being lung, stomach, colorectal, liver and breast cancer [2,3]. It is found that generally cancer risk rises with old age [4]. Colon cancer is now a common malignancy in various parts of the world. Numerous cell-signaling pathways have pivotal roles to play in the proliferation of malignant cells. The search for newer avenues in the treatment of cancer has led research into the elucidation of signaling pathways. The complexity associated with this disease has led scientists to identify targets for the different phases of tumor formation via cell differentiation, proliferation, cell cycle

Abbreviations: ACF, aberrant crypt foci; AO/EB, acridine orange/ethidium bromide; CPCSEA, Committee for the Purpose of Control and Supervision of Experiments on Animals; CMC, carboxymethylcellulose; DMEM, Dulbecco's minimum essential media; DMSO, dimethyl sulfoxide; DMH, 1,2-dimethyl hydrazine; FBS, fetal bovine serum; 5-FU, 5-fluorouracil; HDAC, histone deacetylase; HDACi, HDAC inhibitors; HepG2, human liver adenocarcinoma; HCT 116, human colon adenocarcinoma; IL-6, interleukin-6; *i.p.*, intra-peritoneal; MCF-7, human breast (ER+) adenocarcinoma; MDA-MB-231, human breast (ER−) adenocarcinoma; MTT, 3-(4,5-dimethylthiazol-2-yl)-2,5-diphenyltetrazolium bromide; NCE, new chemical entity; NO, nitric oxide; OECD, Organization for Economic Co-operation and Development; PC3, human prostate adenocarcinoma; PBS, phosphate buffer saline; PI, propidium iodide; *p.o.*, per oral; S.E.M., standard error of mean; SAHA, suberoyl anilide hydroxamic acid; SH-SY5Y, human neuroblastoma; TNF-α, tumor necrosis factor-α; Vero, African green monkey kidney epithelial cell line.

* Corresponding author. Tel.: +91 0820 2922482 (O).
E-mail addresses: mallikin123@gmail.com, mallik.rao@manipal.edu (C. Mallikarjuna Rao).

http://dx.doi.org/10.1016/j.cbi.2015.03.015
0009-2797/© 2015 Published by Elsevier Ireland Ltd.

check point defect, migration and cell survival through onco-gene activation etc. [5].

Cancer is caused by abnormal epigenetic modifications in addition to multiple genetic mutations. Certain validated targets such as tyrosine kinase, farnesyl transferase, histone deacetylase (HDAC), aromatase, etc. play a central role in the development of target specific anticancer agents. Histone deacetylase (HDAC) enzyme overexpression, linked to many cancer types, is responsible for tumor suppressor gene silencing and activation of proto-oncogenes. The altered expression of HDACs play a direct or indirect role in tumor development [6]. HDAC inhibitors (HDACi), a new class of anti-cancer agents, play a crucial role in epigenetic modification, activation of tumor suppressor genes, cell cycle regulation and apoptosis induction in cancer cells. Several HDACi are under pre-clinical or clinical trials. The limitations of these molecules include thrombocytopenia, cardiac problems and poor efficacy against solid tumors etc. [7]. Thus, there is a scope to improve their safety and efficacy.

From time immemorial, use of Tolu balsam as an anti-inflammatory and anti-cancer agent has been well documented owing to the presence of esters of benzoic and cinnamic acid [8]. In recent studies, cinnamic acid derivatives showed anti-cancer activity via HDAC enzyme inhibition [9]. Based on these findings, we made modifications in the cinnamic acid moiety to obtain cinnamyl sulfonamide hydroxamate derivatives. The design evolved around the concept of bio-isosterism and was used as a tool in lead modification [10]; where, the benzene ring of the known available HDACi such as SAHA/PDX101, was conveniently replaced by electronically equivalent ring counterpart such as thiophene. The biological activities of these newly formed NCEs were compared with their phenyl counterparts. Hence, the aim of the present study was to synthesize novel cinnamyl sulfonamide-hydroxamate derivatives and evaluate them for anti-cancer efficacy by *in vitro* and *in vivo* colon adenocarcinoma models.

2. Materials and methods

2.1. Common chemicals and reagents

Starting materials of synthetic grade were obtained from (Sigma–Aldrich Co. LLC, St. Louis, MO, USA; Merck KGaA, Darmstadt, Germany; Spectrochem Pvt. Ltd., Mumbai, MH, India; TCI Co. Ltd., Tokyo, Japan). Dulbecco's modified Eagle's medium (DMEM), phosphatase inhibitor cocktail, protease inhibitor cocktail, propidium iodide (# P4170), SAHA (# SML0061), Boc-Lys(Ac)-AMC substrate (# SCP0168) and Nonidet-P 40 (NP-40), Griess' reagent (# 03553), vanadium (III) chloride (# 208272) were obtained from Sigma–Aldrich Co. LLC, MO, USA; fetal bovine serum (FBS) (Gibco; # 10437036) was obtained from Invitrogen BioServices India Pvt. Ltd., Bangalore, KA, India; 5-fluorouracil (5-FU) was procured from Biochem Pharmaceutical Industries Ltd., Mumbai, MH, India. All chemicals and buffers for Western blotting were obtained from Bio-Rad Laboratories Inc., Hercules, CA, USA. Bax (# 2772S), Bcl-2 (# 2876S), GAPDH (# 2118S), Anti-rabbit IgG HRP-linked (# 7074S) antibodies were procured from Cell Signaling Technology Inc., Danvers, MA, USA. Tissue culture plastic wares and materials were purchased from Tarsons Products Pvt. Ltd., Bangalore, KA, India; Muse™ Annexin V & Dead Cell Kit (Cat# MCH100105), Muse™ Caspase-3/7 Kit (# MCH100108) (Merck KGaA, Darmstadt, Germany); 1,2-dimethylhydrazine hydrochloride [DMH] (# D0742) from TCI Co. Ltd., Tokyo, Japan; IL-6 ELISA kit (# KRC3011), TNF-α ELISA kit (# KRC3011) was purchased from Invitrogen BioServices India Pvt. Ltd., Bangalore, KA, India. All other reagents, chemicals and solvents used in study were of analytical grade quality.

2.2. Equipment for synthesis and characterization of synthesized compounds

Melting point of the synthesized test compounds were determined using capillary melting point apparatus (Toshniwal Systems and Instruments Pvt. Ltd., Chennai, TN, India). The reaction status was checked by TLC on pre-coated silica gel plates (Merck # 60F254). Spots were visualized under both long and short UV range using UV lamp (366 or 254 nm) and iodine chamber. The R_f values for the synthesized test compounds were determined using chloroform: methanol (9:1) solvent system. Further, the test compounds were purified by silica gel column chromatography. The IR spectra were recorded using IR spectrometer (Model FTIR-8300, Shimadzu Co., Kyoto, Japan) using KBr pellets. ^{1}H and ^{13}C NMR were recorded at 400 MHz (Model Ascend 400, Bruker Biosciences Corporation, Billerica, MA, USA) using DMSO (D6) as solvent. Mass spectra were recorded using LC-MS (ESI) (Model LCMS-2010A, Shimadzu Co., Kyoto, Japan). CHN-S elementary analyses were done by Vario EL Ver III CHNS analyzer from Elemental Analysensysteme, GmbH, Germany. NMR, Mass spectra and CHN-S analysis fully supported the final structures of the test compounds. Purity of the test compounds was established on RP-HPLC unit (Shimadzu Co., Kyoto, Japan) with a PDA detector (254 nm) using a Hichrom C18 (250 × 4.6 mm i.d., 5 μm) column with acetonitrile as solvent in pump A and aqueous solution of 0.1% formic acid (pH 6.0) as solvent in pump B by gradient elution. Flow rate of 1.0 ml/min was maintained with a run time of 35 min and column temperature of 30 °C.

2.3. Cell culture and maintenance

All the cell lines (HCT 116, MCF-7, MDA-MB-231, HepG2, SH-SY5Y and Vero) were procured from the National Centre for Cell Science, Pune, MH, India. The cells were maintained in high glucose DMEM medium with 10% FBS and 1% penicillin–streptomycin, at 37 °C in a CO_2 incubator (NU-5510E, NuAire Inc., Plymouth, MN, USA). Trypan blue dye exclusion method was used to check viability of cells and >95% viable cells in culture were used through the experiments. The MTT cell viability assay was performed in all 6 cancer cell lines and rest of the *in vitro* studies were done in HCT 116 colon cancer cell line. Three independent experiments in triplicates were done for the all *in vitro* procedures ($n = 3$).

2.4. Animals, dose administration and treatments

Wistar rats (120–150 g) were used in the study from well-maintained in-house bred, of the Central Animal Research Facility, Manipal University, Manipal, Karnataka, India. All animal experiments were conducted according CPCSEA guidelines, Government of India and after obtaining the experimental protocol approval (No. IAEC/KMC/19/2012) from the Institutional Animal Ethics Committee (Animal Use and Care Committee). Animals were acclimatized in polypropylene cages in experimental room and given standard food pellet rodent diet and water *ad libitum* and kept under controlled humidity conditions 45–55%, temperature 25 ± 2 °C, ventilation 10–12 exchanges/h and 12:12 h light and dark cycle. 5-FU was used as standard drug at a dose of 10 mg/kg, *i.p.* injection which is one twenty fifth (1/25th) of human dose, converted to the rat dose (Paget and Barnes, 1964). NMJ-2 dose was selected based on acute toxicity study limit test (up to 2000 mg/kg). One twentieth (1/20th) of the maximum tested safe dose, i.e. 100 mg/kg was selected for anti-cancer study and administered for a period of 21 days. All other test compounds were prepared as suspensions in 0.25% carboxymethylcellulose (CMC) and administered through oral route.

Please cite this article in press as: N.D. Reddy et al., *In vitro* and *in vivo* evaluation of novel cinnamyl sulfonamide hydroxamate derivative against colon adenocarcinoma, Chemico-Biological Interactions (2015), http://dx.doi.org/10.1016/j.cbi.2015.03.015

2.5. General synthetic procedure for cinnamyl sulfonamide hydroxamate derivatives

2.5.1. Synthesis of (E)-3-(4-(chlorosulfamoyl)phenyl)acrylic acid

Cinnamic acid **1** (Fig. 1) (0.05 mM) and chlorosulfonic acid (0.5 M) were stirred at 35 °C for 4 h. Pre-coated TLC plates were used to monitor the reaction progress. The viscous reaction mixture was poured into ice cubes contained in a beaker. The yellow-colored precipitate that was formed was filtered, washed with distilled water and dried in *vacuo* (anhydrous $CaCl_2$). The crude product was recrystallized from dioxane as **2** (Fig. 1) [11].

2.5.2. Synthesis of (E)-3-(4-(N-(2-(thiophen-2yl) methyl) or (thiophen-2yl)ethyl) or furan-2yl)methyl) sulfamoyl)phenyl)acrylic acid

To a suspension of **2** (Fig. 1) (7.7 mM) in distilled water, thiophene methyl amine (7.7 mM) or thiophene ethyl amine or furfurylamine was added and maintained at pH 8 with aqueous $NaHCO_3$. The reaction mixture was stirred at 35 °C for 4 h. The mixture was then brought to pH 2 by the drop wise addition of 12 M HCl. The product **3** (Fig. 1) obtained as a white precipitate was washed, dried and recrystallized [12].

2.5.3. Synthesis of (E)-N-hydroxy-3-(4-(N-(thiophen-2yl)methyl) or (thiophen-2yl)ethyl) or furan-2yl)methyl)sulfamoyl)phenyl)-acrylamide

To a suspension of **3** (Fig. 1) (10 mM) in dichloromethane (Cl_2CH_2), ethylchloroformate (12 mM) and N-methylmorpholine (13 mM) were added under anhydrous condition using calcium chloride guard tube and the reaction mixture was then stirred at 35 °C for 5 h. The complete conversion of acrylic acid to acid chloride was monitored on pre-coated TLC plates. The simultaneous reaction of conversion of acid chloride to hydroxamate was completed by adding neutral solution of hydroxylamine in tetrahydrofuran (THF) solvent and the reaction mixture was then stirred at 35 °C for 2 h and further partitioned between ethyl acetate and 2 M HCl. The ethyl acetate layer was washed successively with distilled water and evaporated. The residue was purified by silica gel column chromatography to obtain final product **4** (Fig. 1) [13].

2.6. Characterization of cinnamyl sulfonamide hydroxamate derivatives

2.6.1. (E)-N-hydroxy-3-(4-(N-(thiophen-2yl)methyl)sulfamoyl)phenyl) acrylamide [NMJ-1]

Yield = 76%. m.p. uncorrected 178 ± 2 °C; R_f value 0.70. IR (KBr); 3284 (OH), 3209 (N—H 2°), 1672 (C=O carboxylic), 1313, 1180 (O=S=O), 690 (C—S) cm^{-1}, respectively. ^1H NMR (400 MHz, DMSO(D6)) δ 10.87 (1H, s), 9.1(1H, s), 8.3–7.7 (3H, m), 7.5–6.8 (4H, m), 6.6 (1H, d), 6.5 (1H,d), 4.1(3H,s), 1.20 (1H,d) ppm; ^{13}C NMR (400 MHz, DMSO(D6)) δ 162.6 (N—C=O), 141.04 (C—S), 137.1 (C—S), 128.5–126.1 (6C—C), 41.74 (C—N) ppm; CHN-S Elemental analysis: C – 54.28% H – 4.57% N – 8.22% S – 20.51% MS (ESI): m/z = 339.0

2.6.2. (E)-N-hydroxy-3-(4-(N-(thiophen-2yl)ethyl)sulfamoyl)phenyl)-acrylamide [NMJ-2]

Yield = 74%. m.p. uncorrected 150 ± 2 °C; Rf value 0.65. IR (KBr); 3288 (OH), 3205 (N—H 2°), 1691 (C=O carboxylic), 1334, 1168 (O=S=O), 692 (C—S) cm^{-1}, respectively. ^1H NMR (400 MHz, DMSO(D6)) δ 8.32 (1H, s), 7.79 (1H, s), 7.49–7.29 (3H, m), 6.93–6.84 (4H, m), 6.61 (1H, d), 6.51 (1H,d), 4.15(2H,s), 3.9 (2H,s) 1.15 (1H,d) ppm; ^{13}C NMR (400 MHz, DMSO(D6)) δ 162.1 (N—C=O), 140.9 (C—S), 138.9 (C—S), 128.3–125.5 (6C—C), 44.32 (C—N) ppm; CHN-S Elemental analysis: C – 49.02% H – 6.64% N – 7.0% S – 18.29% MS (ESI): m/z = 350.9

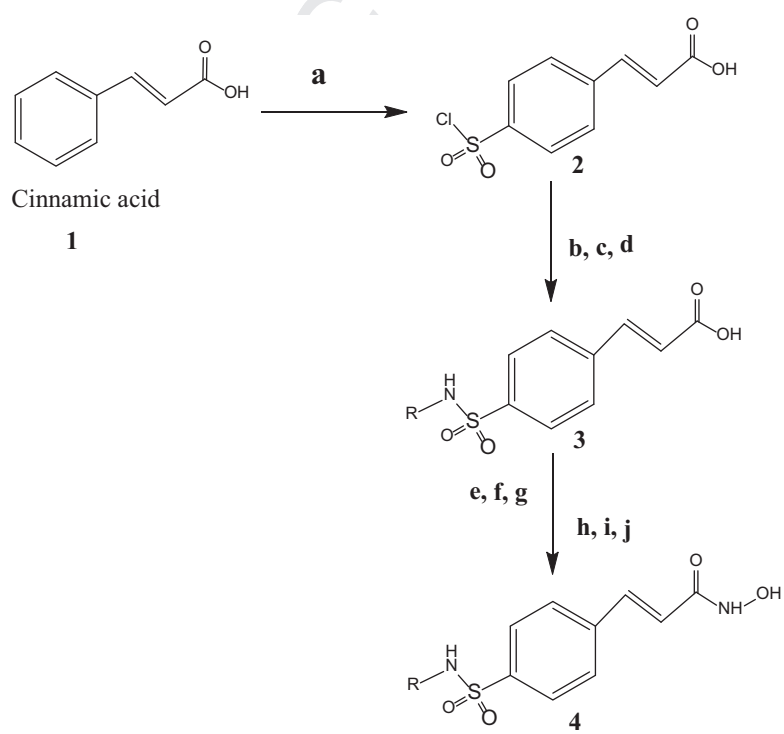

Fig. 1. Synthesis scheme of (E)-N-hydroxy-3-(4-(N-(2-(thophen-2yl)ethyl) sulfamoyl)phenyl)acrylamide. Reagents and conditions: (a) chlorosulfonic acid; stirred mixture at 35 °C for 4 h, (b) thiophene ethyl amine or thiophene methyl amine or furfurylamine, (c) double distilled water, (d) aq. Na_2CO_3; pH maintained at 8 and stirred for at 35 °C for 4 h, (e) ethylchloroformate, (f) CH_2Cl_2, (g) cat. N-methylmorpholine; maintained anhydrous condition and stirred 5 h, (h) NH_2OH, (i) CH_3OH and (j) aq. NaOH; stirred mixture for 2 h.

Please cite this article in press as: N.D. Reddy et al., *In vitro* and *in vivo* evaluation of novel cinnamyl sulfonamide hydroxamate derivative against colon adenocarcinoma, Chemico-Biological Interactions (2015), http://dx.doi.org/10.1016/j.cbi.2015.03.015

2.6.3. (E)-N-hydroxy-3-(4-(N-(furan-2yl)methyl)sulfamoyl)phenyl)-acrylamide [NMJ-3]

Yield = 78%. m.p. uncorrected 138 ± 2 °C; R_f value 0.63. IR (KBr); 3289 (OH), 3209 (N—H 2°), 1685 (C=O carboxylic), 1327, 1180 (O=S=O), 695 (C—S) cm^{-1}, respectively. ^1H NMR (400 MHz, DMSO(D6)) δ 10.92 (1H, s), 9.2 (1H, s), 8.2–7.87 (3H, m), 7.7–6.6 (4H, m), 6.5 (1H, d), 6.2 (1H,d), 4.03 (3H,s), 1.23 (1H,d) ppm; ^{13}C NMR (400 MHz, DMSO(D6)) δ 166.9 (N—C=O), 150.2 (C—S), 142.7 (C—S), 128.6–126.7 (6C—C), 40.1 (C—N) ppm; CHN-S Elemental analysis: C – 42.97% H – 3.62% N – 5.93% S – 8.06% MS (ESI): *m/z* = 320.9

2.7. Cell culture and treatment

2.7.1. Cell viability study by MTT assay

In brief, 70% confluent cultured flask containing 5×10^3 cells/100 μl cells were plated in 96-well plates and allowed to attach cells at bottom by keeping plates overnight in incubator. Then cells were exposed to different concentrations of compound for 48 h. After the incubation, MTT reagent 10 μl (5 mg/ml in PBS) was added and cells incubated for an additional 3 h. The formazan crystals formed by the viable cells were solubilized by addition of DMSO and plate absorbance was measured at 540 nm using microplate ELISA reader (ELx800, BioTek Instruments Inc., Winooski, VT, USA) [14]. The IC_{50} for compound was determined by using Prism 5.03 Demo Version (GraphPad Software Inc., La Jolla, CA, USA).

2.7.2. Whole cell HDAC enzyme assay

In brief, 2×10^4 cells were seeded in 50 μl in 96-well standard sterile black plates and incubated over night at 37 °C with 5% CO_2 in incubator. The cells were incubated for 18 h with different concentration of compounds. Then, 2 μl of 15 mM Boc-Lys(Ac)-AMC substrate was added and incubated for 1 h at 37 °C with 5% CO_2 in an incubator. The reaction was stopped by adding 100 μl HADC assay buffer containing 2 mg/ml of trypsin and 1% NP-40. The reaction was allowed to proceed for 15 min at 37 °C with 5% CO_2 in incubator and the fluorescence was taken at excitation 360 nm and emission 460 nm by using fluorescence microplate reader (FLx800, BioTek Instruments Inc., Winooski, VT, USA) [15]. The IC_{50} for compound was determined by using fully functional Prism 5.03 Demo Version (GraphPad Software Inc., La Jolla, CA, USA).

2.7.3. Hoechst 33342 and AO/EB (dual) nuclear staining

In brief, the 5×10^3 cells/well were seeded in 24-well plates with DMEM containing 10% FBS. After 24 h, cells were treated with different concentration of compounds and incubated for 48 h. The plate was washed with PBS, pH 7.4 and cells were fixed with ice-cold methanol for 20 min. Then cells were washed with PBS again and 300 μl of Hoechst 33342 stain (2 μg/ml) or AO/EB (20/30 μg/ml) was added to each well. The plate was incubated at 37 °C for 20 min. Finally the plate was washed thrice with PBS and observed under a fluorescent microscope (Eclipse TS100-F, Nikon Instruments Inc., Melville, NY, USA) for morphological changes in nucleus like condensed chromatin and fragmented nuclei. The apoptotic index (AI) was calculated as % of apoptotic cells from randomly counted 100 cells in each treatment group [16].

2.7.4. Cell cycle analysis

In brief, the 1×10^6 cells were seeded in 25 cm^2 flasks and after overnight adherence, incubated with test compounds. Then cells were detached by trypsinization and mixed with floating cells, centrifuged and washed with PBS. The cell pellets were fixed in 70% ice-cold methanol and stored at −20 °C for 24 h. After that cell pellets were washed with PBS and isotonic PI solution [25 μg/ml propidium iodide, 0.03% NP-40 and 40 μg/ml RNase A] was added. The stained cells were analyzed using Accuri C6 flow cytometer (BD Biosciences, San Jose, CA, USA) using excitation at 488 nm and emission at 575/40 nm. A minimum of 10,000 events were acquired for each sample and data analysis was done by using BD Accuri™ C6 software [17].

2.7.5. Early and late apoptosis detection by Annexin V staining

In brief, as per Annexin V flow cytometry kit protocol, 1×10^6 cells were seeded in 25 cm^2 flasks and after overnight adherence, incubated with test compounds. Then cells were detached by trypsinization and mixed with floating cells, centrifuged and washed with PBS. Cell suspension (100 μl) was mixed with Muse Annexin V and Dead Cell kit reagent (100 μl) and incubated for 20 min at room temperature. The stained cells were quantitatively analyzed for live, early and late apoptosis and dead by using Muse Cell Analyzer (# 0500-3115 Merck Millipore) with Annexin V kit (# MCH100105 Merck Millipore) [18].

2.7.6. Detection of caspase 3/7 activation

In brief, as per caspase 3/7 activation flow cytometry kit protocol, 1×10^6 cells were seeded in 25 cm^2 flasks and after overnight adherence, incubated with the test compounds. Then cells were detached by trypsinization and mixed with floating cells, centrifuged and washed with PBS. Cell suspension (50 μl) was mixed with Caspase-3/7 antibody reagent (5 μl) and incubated at 37 °C temperature for 30 min. 7-AAD working solution (150 μl) was added and stained cell were analyzed in Muse Cell Analyzer (# 0500-3115 Merck Millipore) with Caspase 3/7 kit (# MCH100108 Merck Millipore) [18].

2.7.7. Western blot analysis

In brief, the whole-cell extract was generated from cell pellets in mammalian protein extraction buffer supplemented with protease and phosphatase inhibitor cocktail. The protein quantification was done by using commercial protein estimation BCA™ kit (Thermo Fisher Scientific Inc., Waltham, MA, USA) and protein samples (20 μg) were dissolved in 5× sample loading buffer and DTT (100 mg/ml) and boiled for 5 min at 99 °C. This was resolved on a 10% SDS–PAGE and blotted on to a PVDF membrane and blocked with 5% non-fat milk protein in TBS-T buffer for 1 h at room temperature. The primary antibodies (anti-rabbit Bax, anti-rabbit Bcl-2 and anti-rabbit GAPDH) were probed overnight at 4 °C. After washing with TBS-T buffer, the horseradish peroxidase–conjugated secondary antibody was subsequently incubated for 1 h at 25 °C room temperature. The signal was visualized by using Pierce enhanced chemiluminescent (ECL) Western Blotting Substrate kit (Thermo Fisher Scientific Inc., Waltham, MA, USA) on medical grade X-ray film [19]. The relative densities were quantified by using calibrated densitometer (GS 800, Bio-Rad

Table 1
List of cinnamyl sulfonamide-hydroxamate derivatives with different substitutions.

S. no.	Compound code	Heteroaromatic amines (R) Name	Structure
1	NMJ-1	Thiophene methyl amine	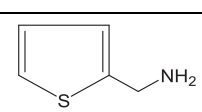
2	NMJ-2	Thiophene ethyl amine	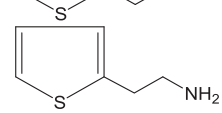
3	NMJ-3	Furfurylamine	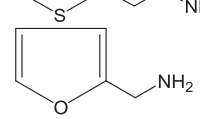

Laboratories Inc., and Hercules, CA, USA) with Quantity One 1D analysis software.

2.8. In vivo studies

2.8.1. Acute toxicity studies

The safe dose was determined according to OECD-425; Limit test dose (2000 mg/kg) was given *p.o.* to fasting female rats. Animals were observed for toxic signs for the first 4 h continuously and then daily observed for 14 days.

There was no mortality with 2000 mg/kg dose of NMJ-2. The external morphological, behavioral, neurological profile was found to be normal. Thus, NMJ-2 passed limit test and was found to be safe up to 2000 mg/kg dose level. So, 1/20th dose, i.e. 100 mg/kg, *p.o.* was selected for efficacy studies.

2.8.2. DMH (1,2-dimethyl hydrazine) induced colon cancer in Wistar rats

2.8.2.1. Experimental design. Animals were divided into 4 groups and dose was administered as follows:

- Normal control (sham control)
- DMH control [0.25% CMC, *p.o.* 10 ml/kg and saline *i.p.* 1 ml/kg] (DMH + vehicle)
- Standard drug (5-FU injection; 10 mg/kg, *i.p.*) (DMH + 5-FU)
- Test compound (NMJ-2; 100 mg/kg, *p.o.*) (DMH + NMJ-2)

2.8.2.2. Procedure. In brief, animals (Wistar rats) in the weight range of 120–150 g were taken for study. DMH (1,2-dimethyl hydrazine) 30 mg/kg body weight was given by *i.p.*, once a week, for 20 weeks [20]. After 20 weeks one animal from each group was sacrificed and observed for incidence of aberrant crypt foci (ACFs) and adenocarcinoma. Animals were randomized on the basis of equal mean body weight throughout the groups and test compound and standard drug were administered for 21 days. At the end of the study, rats were sacrificed humanely and colons were excised, blotted and dried. The following parameters were estimated.

- ACF, adenocarcinoma incidence and count
- Biochemical parameters
- Organ index
- Hematological parameters
- Histopathology of colon

2.8.2.3. ACF, adenocarcinoma incidence and count. Initially, the entire colon was observed for adenocarcinoma. If present, the count and size from each animal was noted. The distal colon tissue (5 cm^2) was cut open and fixed flat on filter paper and fixed with 10% buffered formalin for 12 h and then stained with 0.1% of methylene blue in PBS for 5 min. Specimens were observed under stereo microscope (40× magnification). ACFs were clearly defined as microscopically elevated slit-like opening with a thick epithelial lining that deeply takes up the stain in the vicinity of the cryptal zone that was larger than normal crypts. ACF were counted and calculated as number of counts/5 cm^2 [21].

Table 3
Effect of NMJ-1, 2, 3 and SAHA incubated for 18 h, on whole cell HDAC enzyme and its correlation with apoptotic protein expression such as phosphatidylserine (Annexin V), Bax/Bcl-2 ratio and activated caspase 3/7 in HCT 116 cells.

S. no.	Compound name	Whole cell HDAC inhibition IC_{50} (μM ± SEM)	Phosphatidylserine (Annexin V) (% early apoptosis)	Bax/ Bcl-2 ratio	Caspase 3/7 (% apoptosis)
1	Normal control	–	4.8	0.308	21.55
2	5-FU	–	13.95	1.010	56.10
3	SAHA	2.63 ± 0.07	14.30	1.573	43.50
4	NMJ-1	3.89 ± 0.17	–	–	–
5	NMJ-2	0.41 ± 0.01	12.0	1.708	79.75
6	NMJ-3	5.85 ± 0.79	–	–	–

2.8.2.4. Biochemical parameters. 10% homogenate of colon tissue was prepared in ice cold mammalian tissue lysis buffer supplemented with protease and phosphatase inhibitor cocktail using a homogenizer (RQ-124A/D, REMI Laboratory Instruments, Mumbai, India). The homogenate was centrifuged by using cooling centrifuge (MIKRO 22R, Andreas Hettich GmbH & Co.KG, Tuttlingen, Germany) at 14,000 rpm for 10 min at 4 °C and the pellets were discarded. The supernatant was used for total protein estimation, using BCA™ commercial kit (Thermo Fisher Scientific Inc., Waltham, MA, USA), TNF-α (ELISA kit # KRC3011, Invitrogen) and IL-6 (ELISA kit # KRC3011, Invitrogen) [22], nitrite and nitrate estimation.

Nitrite, total nitrate + nitrite contents were estimated by Griess' reagent method, adopting the established procedure [23,24]. Nitrate was reduced into nitrite by using acidic solution of vanadium (III) chloride and mild heat.

Nitrite estimation: 100 μl of Griess' reagent and 100 μl of supernatant were incubated at 37 °C in 96 well plates for 20 min and absorbance was measured at 540 nm. The amount of nitrite was quantified from sodium nitrite standard curve.

Total nitrate + nitrite estimation: 100 μl of Griess' reagent, 100 μl of supernatant and 100 μl of vanadium (III) chloride (0.8% in 1 N HCl) were incubated in microcentrifuge tubes at 45 °C for 60 min. 100 μl of each of the samples were added into 96 well plates and absorbance was measured at 540 nm.

Nitrate contents were calculated by subtracting nitrite values from total nitrate + nitrite contents.

2.8.2.5. Organ index. Colons were isolated, length was measured in cm and weight was measured in g and the colon weight/length

Table 2
Effect of treatments on the proliferation of different cells after 48 h.

S. no.	Cell line	Cytotoxicity assay compound incubation time for 48 h IC_{50} (μM ± SEM)				
		5-FU	SAHA	NMJ-1	NMJ-2	NMJ-3
1	HCT 116	22.0 ± 0.35	3.1 ± 0.35	5.07 ± 0.9	3.3 ± 0.15	17.3 ± 0.9
2	MCF-7	23.7 ± 2.2	5.2 ± 0.1	5.3 ± 0.3	5.5 ± 0.3	26.8 ± 2.0
3	MDA-MB-231	33.4 ± 1.1	3.8 ± 0.25	4.4 ± 0.2	3.9 ± 0.3	21.7 ± 1.7
4	HepG2	8.8 ± 0.8	11.7 ± 1.1	9.8 ± 1.3	4.1 ± 0.6	44.9 ± 2.6
5	PC3	30.2 ± 0.47	2.4 ± 0.3	5.6 ± 0.5	5.8 ± 0.2	18.6 ± 0.9
6	SH-SY5Y	5.3 ± 0.43	4.7 ± 0.52	4.5 ± 0.6	3.6 ± 0.3	20.1 ± 0.42
7	Vero	45.0 ± 3.0	5.1 ± 0.2	9.7 ± 1.7	8.2 ± 1.0	15.1 ± 1.5

Please cite this article in press as: N.D. Reddy et al., *In vitro* and *in vivo* evaluation of novel cinnamyl sulfonamide hydroxamate derivative against colon adenocarcinoma, Chemico-Biological Interactions (2015), http://dx.doi.org/10.1016/j.cbi.2015.03.015

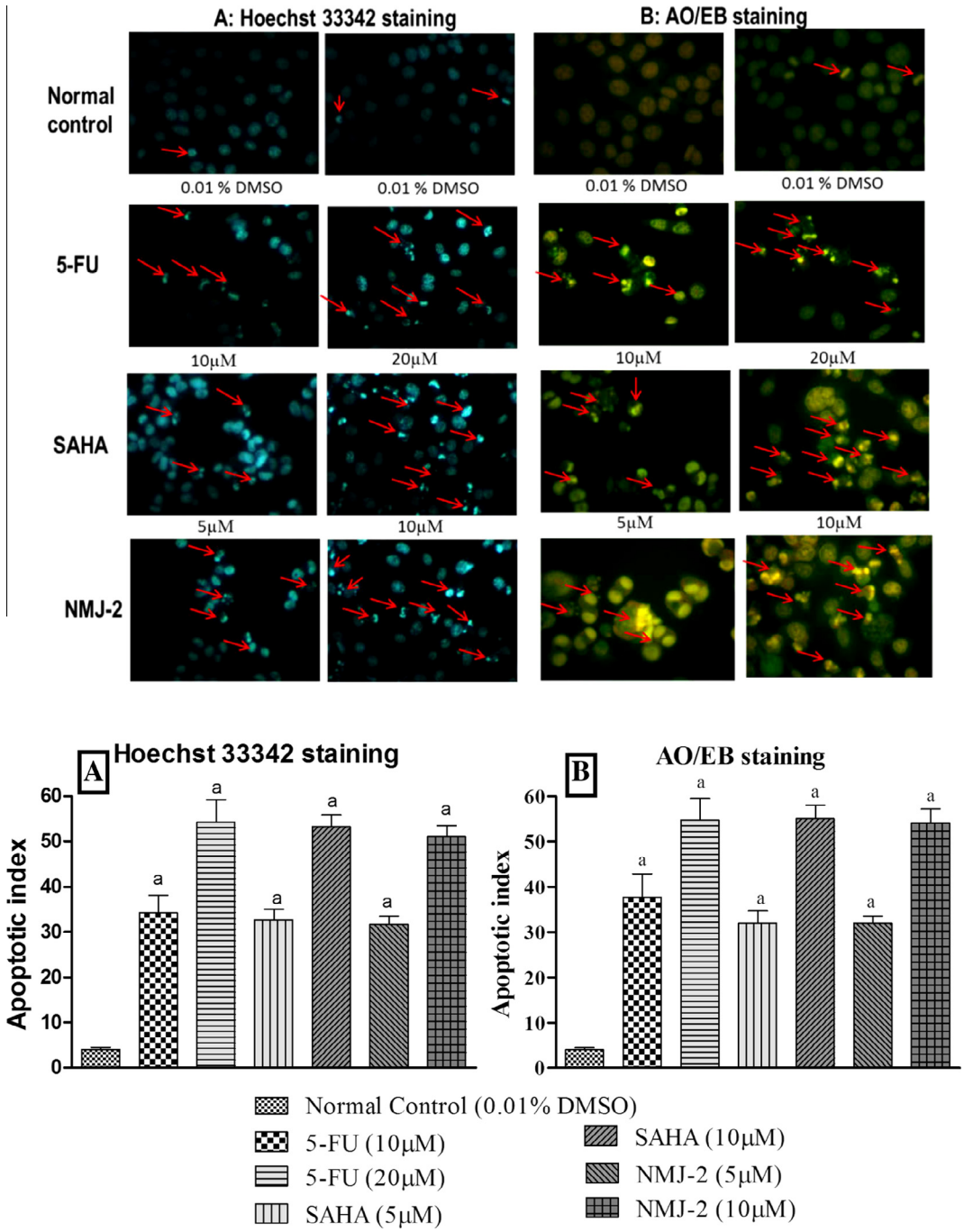

Fig. 2. The representative images for induction of apoptosis by different treatments for 48 h in HCT 116 cells. Apoptotic index was calculated by counting specific pattern of condensed and fragmented nuclear morphology. Figure A: Hoechst 3342 staining, B: AO/EB staining. Graph A: Hoechst 3342 staining, B: AO/EB staining. All values are mean ± SEM of three samples, $^{a}p < 0.05$ vs normal control.

ratio was calculated. Spleen and liver were isolated, weighed in g and spleen index and liver index were calculated.

2.8.2.6. Hematological parameters. Blood was collected into di-potassium EDTA-coated vacutainers from the retro-orbital plexus and analyzed for various circulatory blood cells by using veterinary blood cell counter (Model PCE-210 VET, ERMA Inc., Tokyo, Japan).

2.8.2.7. Histopathology of colon. The colon tissue was fixed in 10% neutral buffered formalin for 24 h and dehydrated with alcohol. The tissue was then cleared in xylene and paraffin-embedded. Five micron thick sections were cut using a rotary microtome (RM2245, Leica Microsystems GmbH, Wetzlar, Germany). Sections were spread in a temperature regulated tissue float (Model 375, Lipshaw Manufacturing Corporation, Detroit, MI, USA) and fixed on clean slides pre-coated with egg albumin. The sections were stained with methylene blue, Harris hematoxylin, counter stained with eosin and mounted in DPX and scored for gross anatomical and histopathological changes.

2.8.2.8. Statistical analysis. Statistical analysis of the data was done by one-way ANOVA followed by the Tukey's post hoc test using fully functional Prism 5.03 Demo Version (GraphPad Software Inc., La Jolla, CA, USA). A value of $p < 0.05$ was considered to be significant.

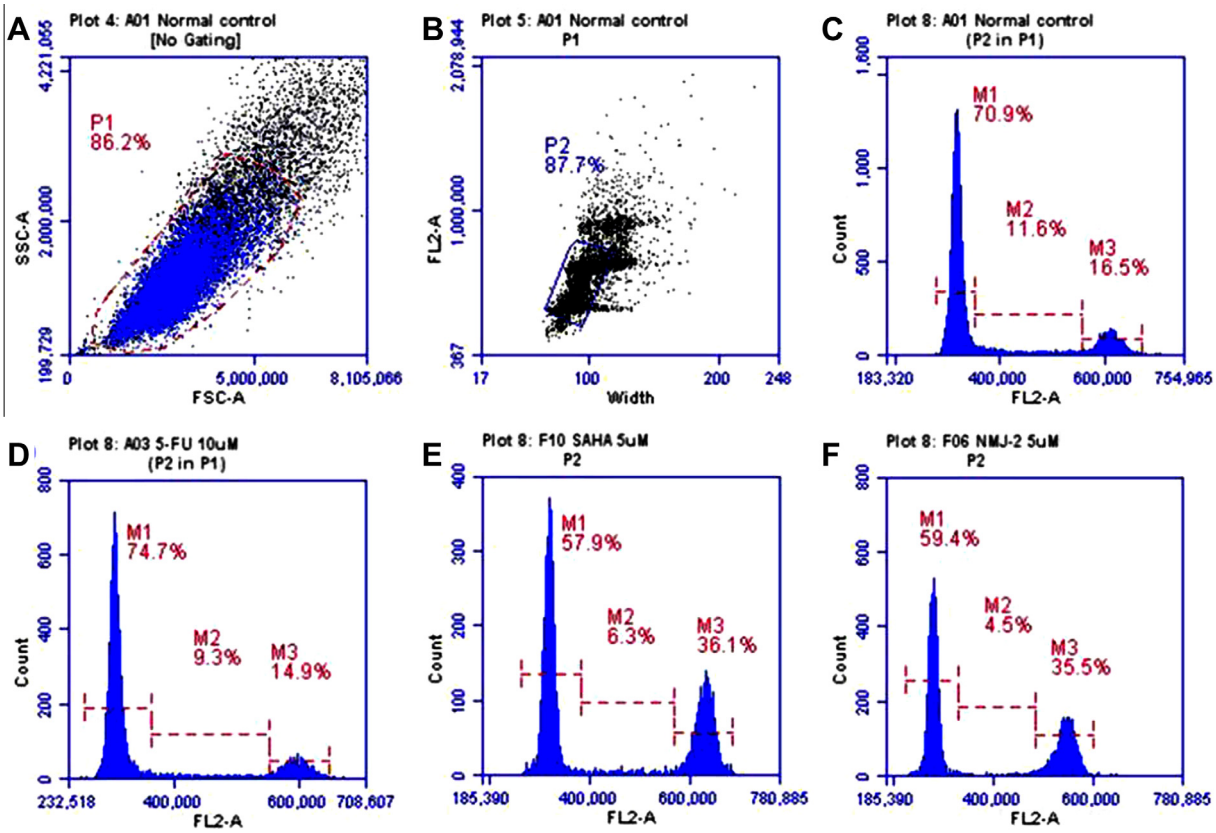

Fig. 3. Effect on the cell cycle of HCT 116 after 48 h treatment. The % cells in specific G_0/G_1, S and G_2/M phase was estimated the by flow cytometry. (A) FSC vs SSC plot for normal control population, (B) width vs FL2-A plot for 2n to 4n normal control gated population, (C) FL2-A vs count histogram plot for normal control (0.01%), (D, E and F) FL2-A vs count histogram plots for 5-FU (10 μM), SAHA (5 μM) and NMJ-2 (5 μM) respectively.

3. Results and discussion

The present study explored the anti-cancer potential of three novel cinnamyl sulfonamide hydroxamate derivatives [NMJ series] against the target enzyme, HDAC by a series of *in vitro* and *in vivo* screening models of colon adenocarcinoma. A number of different approaches were adopted to establish the anti-cancer and anti-inflammatory effects of NMJ-2, which showed the maximum efficacy out of the three tested compounds.

A number of targets have multiple roles in the complexities of carcinogenesis, which may be biochemically mediated, genetically predisposed and epigenetically controlled. Overexpressed HDAC is responsible for sustaining the levels of deacetylated histones, which in turn, are responsible for activation of tumor promoter gene and inactivation of tumor suppressor genes [7]. This was selected as a target for the development of newer therapies (Table 1).

3.1. Cell viability study by MTT assay

The pre-requisite for any chemical scaffold to show anti-cancer activity is that the compounds should primarily be cytotoxic to cancer cells. Generally anti-cancer activity of the test compounds is primarily evaluated by their cytotoxic potential in different types of cancer cell lines. The anti-cancer potential of NMJ-1, 2, 3 was evaluated against six different human cancer cell lines *in vitro* by MTT cytotoxicity assay after 48 h of incubation with the following drugs viz. 5-FU, SAHA and test compounds NMJ-1, 2, 3 is shown in Table 2. The three test compounds NMJ-1, 2, 3 showed growth inhibition IC_{50} at a range of 3.3 ± 0.15–44.9 ± 2.6 μM. NMJ-2, was more cytotoxic than 5-FU and comparable with that of SAHA. NMJ-2 was more active against HCT 116 (highly metastatic) with its IC_{50} of 3.3 ± 0.15 μM and had 2.5-fold selectivity towards human colon adenocarcinoma cells (HCT 116) over normal kidney epithelial cells (Vero). The above result showed its selective cytotoxicity towards cancerous cells compared to normal cells.

3.2. Whole cell HDAC enzyme assay

The interaction of HDAC enzyme with associated protein, mainly histone, present in intact nuclei of cells, is a complex physiological process. However, isolated, recombinant and purified enzyme interaction solely with the test compound will not give any clear picture regarding the natural protein–protein interactions. To overcome this limitation, whole cell HDAC assay provides a better insight in understanding the natural protein–protein interactions in intact cells or tissues and further helps in simulating the physiological system [25]. Thus, the same has been employed in the present study to assess the inhibition activity of the NCEs on HDAC.

The whole cell HDAC enzyme inhibition activity of NMJ-2 (being the most potent one) was compared with that of the standard, SAHA (marketed HDAC inhibitor), as shown in Table 3. A dose dependent HDAC inhibition was clearly observed with NMJ-2. Besides, it had higher potency than the standard SAHA. The whole cell HDAC enzyme inhibition IC_{50} of NMJ-2 and SAHA were about 0.41 ± 0.01 and 2.63 ± 0.07 μM, respectively, as shown in Table 3.

3.3. Hoechst 33342 and AO/EB (dual) nuclear staining

Both the fluorescent nuclear staining dyes have the property of permeation into cells and hence are used to study the morphological features of nuclear DNA or RNA. The mechanism underlying the cell death induced by test compounds in HCT 116 was confirmed

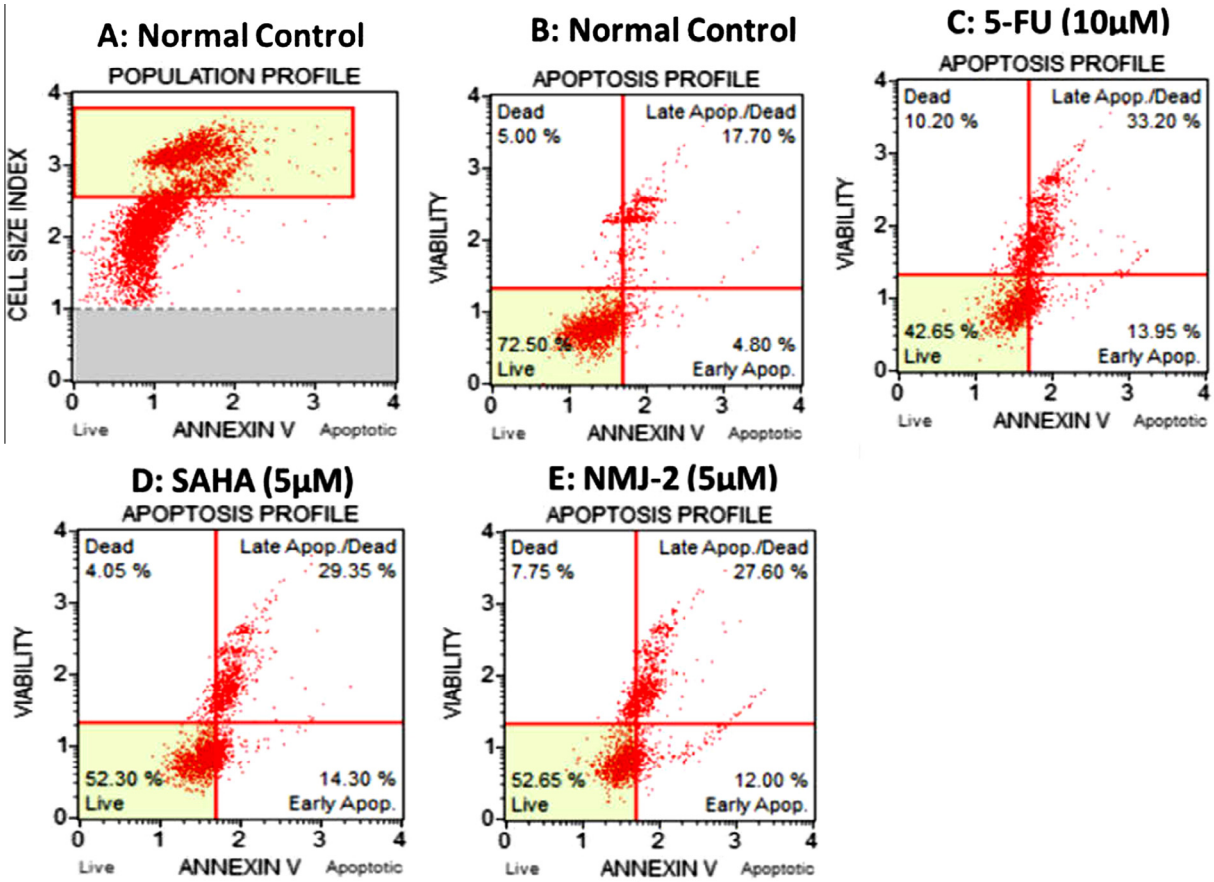

Fig. 4. Effect on Annexin V surface binding in HCT 116 cancer cells after 48 h treatment. Apoptosis profile was assessed as % live, early, late apoptosis and dead cells by flow cytometry. (A) Population profile for normal control (0.01%); (B, C, D and E) Annexin V staining apoptosis profile for normal control, 5-FU (10 µM), SAHA (5 µM) and NMJ-2 (5 µM), respectively.

by these fluorescent dyes. Hoechst 33342 indicates the DNA fragmentation or chromatin condensation whereas AO/EB (dual) staining facilitates visualization of apoptotic changes and/or necrosis. The hallmark features of Hoechst 33342 staining included the presence of fragmented nuclear DNA (seen as visible cluster of blue spots) and condensed chromatin (appear as a bright blue colored intense spot). However, in case of AO/EB stain, the cells appear as green colored distinct spots for viable cells, yellow color for early apoptotic cells and reddish to orange staining for the late apoptotic cells [26].

The normal control (0.01% DMSO) showed the apoptotic index about 3.3 ± 0.88 and 5.0 ± 1.0% with Hoechst 33342 and AO/EB (dual) staining, respectively. Further, NMJ-2 treatment showed dose dependent significant increase in apoptotic index and was comparable with that of the standard SAHA and 5-FU as shown in Fig. 2.

3.4. Cell cycle analysis

The cell cycle involves different phases such as G_0–G_1, S, G_2 and M with check point at G_1 (restriction point), G_2 check point and M (metaphase) check point. These check points play an important role, working as sensors to assess the extent of DNA damage caused by the external factors and facilitate the cell's need to undergo proliferation or apoptosis. If the arrest in the cell cycle continues, it could either repair the damaged DNA or induce apoptosis if the repair of damaged DNA does not happen [27,28].

The effects of the compounds on cell cycle were assessed using flow cytometry and the result of the same was shown as % cells in G_0/G_1, S and G_2/M phase. The normal control showed the distribution of cells in G_0/G_1, S and G_2/M phase as 70.9%, 11.6% and 16.5% cells, respectively. However, the standard drug, 5-FU at 10 µM treatment caused accumulation of cells in G_0/G_1 phase (74.7%), indicating clearly the cell cycle arrest. SAHA (5 µM) and NMJ-2 (5 µM) treatments showed increase in cell population at 36.1% and 35.5% cells, respectively in G_2/M phase (Fig. 3). This is an indication that cell cycle of the cancer cells is arrested in G_2/M phase by the compounds perhaps due to overexpression of negative cell cycle regulators through HDAC inhibition.

3.5. Early and late apoptosis detection by Annexin V staining

Annexin V is a cellular protein exclusively used for staining purpose in the detection of apoptosis. In this method, Annexin V is combined with propidium iodide. Generally Annexin V helps the early detection of apoptosis whereas the combined stain would enable the detection of the late stage of apoptosis. This protein has affinity to bind with the phosphatidylserine (PS) which is located along the cytosolic side of the plasma membrane in healthy cells. Whenever apoptosis is initiated, PS translocates into the extracellular membrane after which Annexin V interacts and thus facilitates the identification of various stages of apoptosis [29]. In the early stages, only Annexin V would bind to the surface protein while in the later stage of apoptosis, there would be loss in the cell membrane integrity allowing Annexin V to further bind to cytosolic PS along with cellular uptake of propidium iodide. These changes are clearly identified by flow cytometry. The test compound, NMJ-2, significantly promoted the early and late stages of

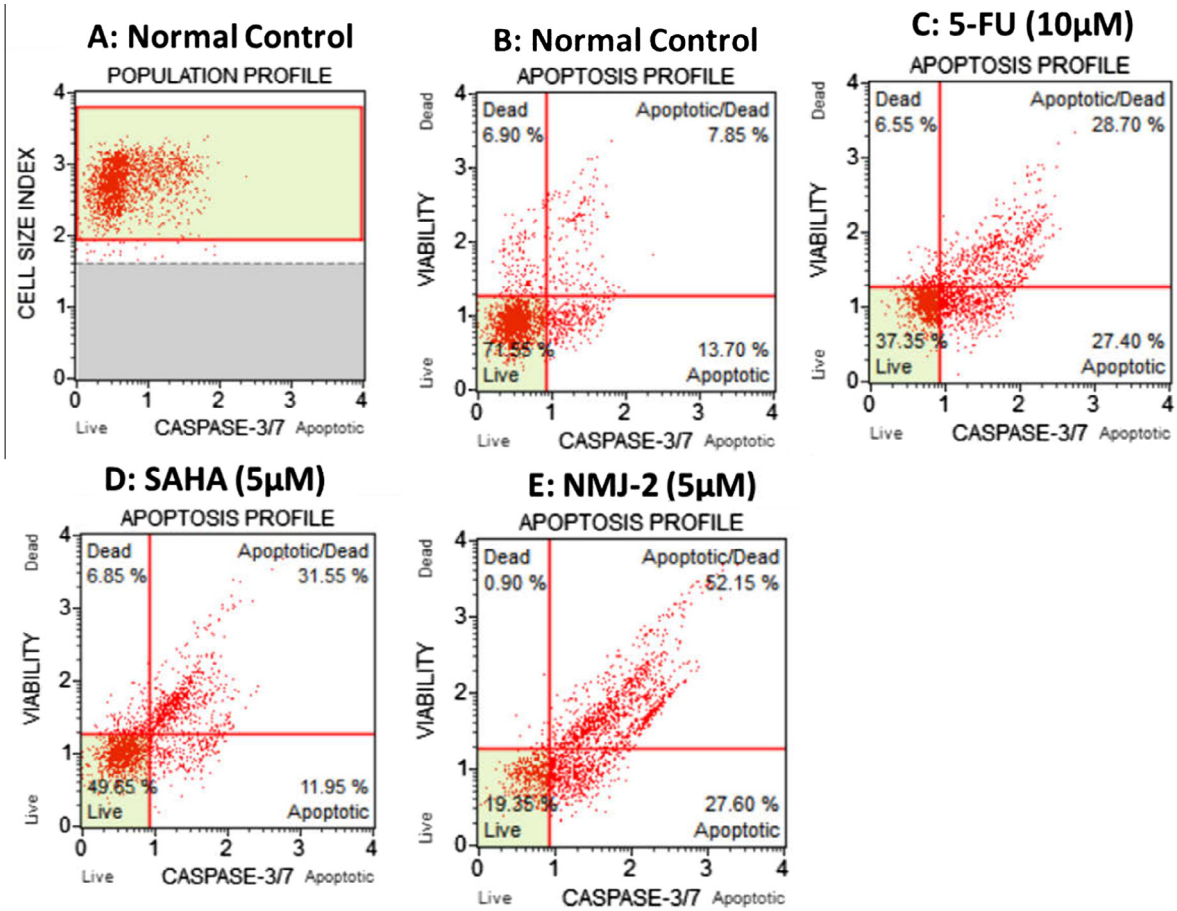

Fig. 5. Effect on caspase 3/7 activation in HCT 116 cancer cells after 48 h treatment. Apoptosis profile was assessed as % live, early, late apoptosis and dead cells by flow cytometry. (A) Population profile for normal control (0.01%); (B, C, D and E) caspase 3/7 activation profile for normal control, 5-FU (10 µM), SAHA (5 µM) and NMJ-2 (5 µM), respectively.

apoptosis and the effects were comparable with that of the standard drugs, SAHA and 5-FU, as shown in the Fig. 4.

3.6. Detection of caspase 3/7 activation

Caspases are the central regulators of programmed cell death. The effector caspase 3/7 activation plays a very important role in the initiation of apoptosis [30]. Our study on caspase activation revealed that the test compound, NMJ-2 increased early and late stages of apoptosis and its activity was comparable with standard drugs, SAHA and 5-FU as shown in the Fig. 5.

3.7. Western blot analysis

Bcl-2 gene family members are the most important regulators of apoptosis. Bax and Bcl-2 have apoptosis induction and inhibition roles, respectively [31]. The pro-apoptotic action of Bax protein is dependent on the formation of Bax homodimers on the outer mitochondrial membrane. The antagonistic effect of Bcl-2 protein is by preventing the formation of Bax homodimers [32]. The cellular Bax/Bcl-2 ratio is a key factor in the regulation of apoptosis; a low Bax/Bcl-2 ratio makes cells resistant to apoptotic signal, while a high ratio induces cell death [32,33]. The Bax protein induces apoptosis through the opening of mitochondrial voltage-gated anion channels [34], which further raises the mitochondrial outer membrane permeability. This leads to the release of cytochrome c that triggers the activation of effector caspases 3 and 7 [35]. In the present study, all the three treatments, i.e. 5-FU, SAHA and NMJ-2 showed a 3-fold increase in Bax expression and 1.2, 1.8 and 1.9-fold decrease in Bcl-2 expression, respectively when compared with that of the normal control. The ratio of Bax/Bcl-2 was increased by 3.2, 5.0 and 5.5 folds with 5-FU, SAHA and NMJ-2, respectively (Fig. 6).

3.8. Correlation of HDAC enzyme inhibition with apoptotic protein expressions

The HDAC enzyme inhibition is correlated with apoptotic protein expression such as phosphatidylserine (Annexin V), Bax/Bcl-2 ratio and activated caspase 3/7. NMJ-2 treatment resulted in HDAC enzyme inhibition which led to increased Bax/Bcl-2 ratio and increased activation of caspase 3/7 leading to apoptosis. The expression levels of phosphatidylserine in NMJ-2 were comparable with that of 5-FU and SAHA. Hence, NMJ-2 seems to be a more potent HDAC inhibitor than SAHA, NMJ-2 and NMJ-3 (Table 3).

3.9. DMH (1,2-dimethyl hydrazine) induced colon cancer in Wistar rats

The development of colon cancer involves three important phases. In the initiation phase, a single mutation leads to the abnormal proliferation of cells. Next, additional mutations lead to the proliferation of selected transformed cells within the population in the promotion phase. Finally, in the progression phase, multiple mutated tumor clone cells produce malignant tumors. Thus, the sequence of events consists of phases for both prevention

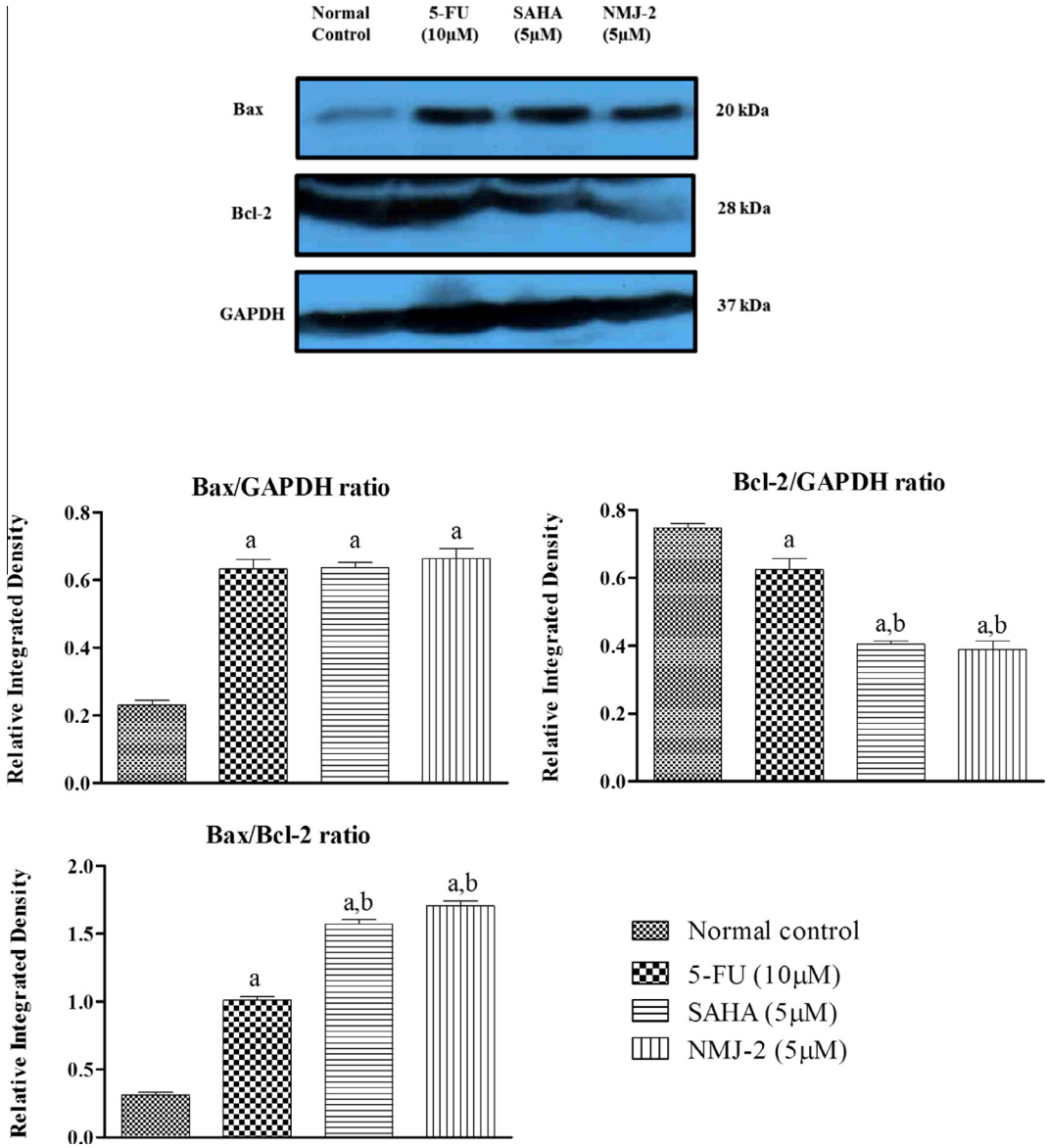

Fig. 6. Effect of 5-FU, SAHA and NMJ-2 incubated for 48 h, on Bax, Bcl-2 protein expression in HCT 116 cells. The relative integrated density of Bax/GAPDH, Bcl-2/GAPDH and Bax/Bcl-2 ratio was calculated using calibrated densitometer with Quantity One 1D analysis software. All values were mean ± SEM of three samples, [a]$p < 0.001$ as compared to normal control and [b]$p < 0.001$ as compared to 5-FU (standard).

Table 4
Effect of DMH + 5-FU (10 mg/kg, *i.p.*) and DMH + NMJ-2 (100 mg/kg, *p.o.*) administration for 21 days on ACF incidence and count; adenocarcinoma count and size (measured by Vernier caliper). All values are mean ± SEM, $n = 6$.

S. no.	Group	ACF incidence (%)	No. of ACF/5 cm^2 (mean ± SEM)	Adenocarcinoma			
				Small ~(0.1–2 mm)	Medium ~(2–4 mm)	Large ~(4–8 mm)	Total
1	Normal control	0	0	0	0	0	0
2	DMH + Vehicle	100.0	84.25 ± 7.6[a]	7	6	4	17
3	DMH + 5-FU (10 mg/kg)	100.0	58 ± 5.0[a,b]	4	3	1	8
4	DMH + NMJ-2 (100 mg/kg)	100.0	64.5 ± 6.7[a,b]	5	2	2	9

[a] $p < 0.05$ vs normal control.
[b] $p < 0.05$ vs DMH control.

and intervention [36]. Further, in human cancer development, gene mutation is associated with chronic inflammation which is considered one of the major risk factor [37].

DMH, a chemical carcinogen, is known to cause colon cancer in a reproducible *in vivo* experimental system for studying sporadic (non-familial) forms of colon carcinoma where, DMH is converted to its final carcinogenic metabolite such as diazonium ions, azoxymethane (AOM) and methylazoxymethanol (MAM) by NAD$^+$-dependent dehydrogenase enzyme. Further, these intermediates, alkylate (methylation) colonic mucosal DNA and generate oxidative stress. This results in a delayed or incomplete repair of damaged DNA leading to the accumulation of multiple mutations

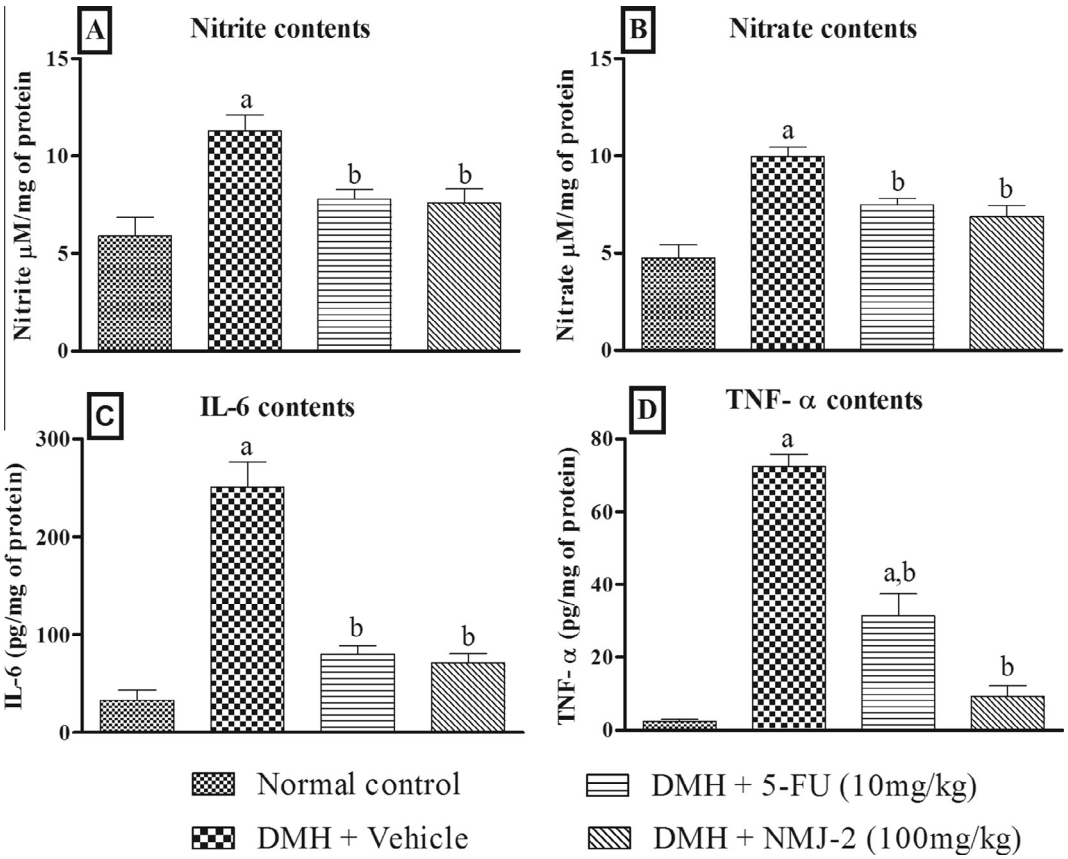

Fig. 7. Effect of DMH + 5-FU (10 mg/kg, *i.p.*) and DMH + NMJ-2 (100 mg/kg, *p.o.*) administration for 21 days on inflammatory markers. (A) Nitrite, (B) nitrate, (C) IL-6 and (D) TNF-α contents in colon tissue homogenate. All values are mean ± SEM of six samples. [a]$p < 0.05$ vs normal control, [b]$p < 0.05$ vs DMH control.

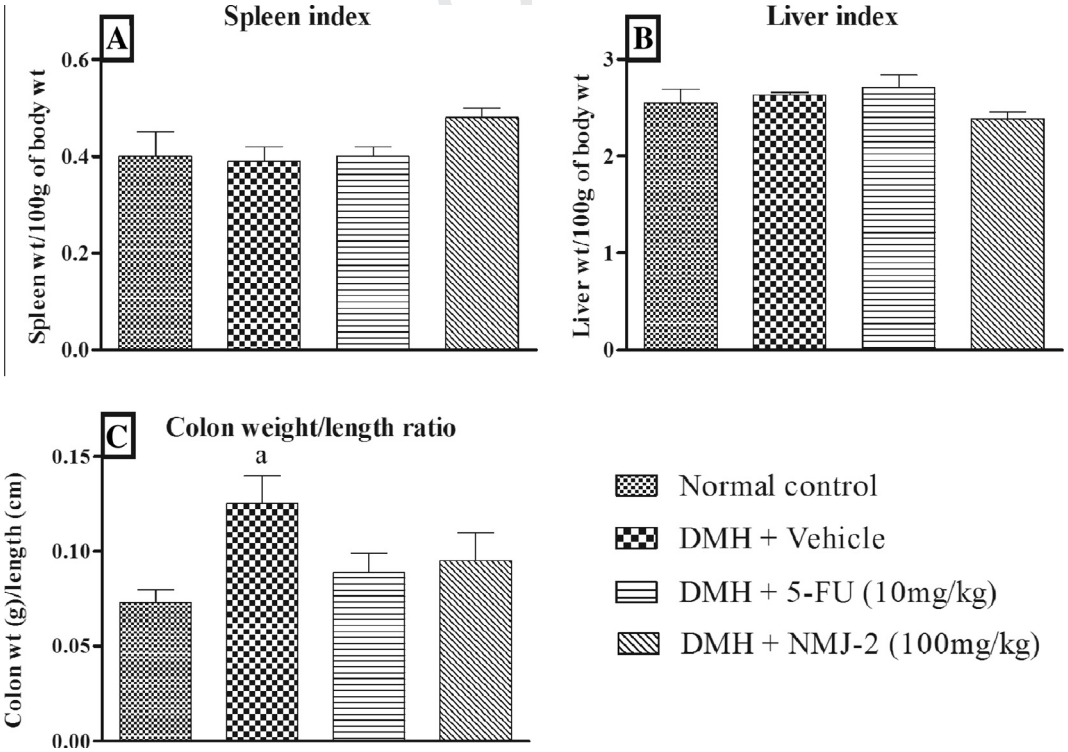

Fig. 8. Effect of DMH + 5-FU (10 mg/kg, *i.p.*) and DMH + NMJ-2 (100 mg/kg, *p.o.*) administration for 21 days on organ index. (A) Spleen index, (B) liver index, (C) colon weight/length ratio. All values are mean ± SEM of six samples. [a]$p < 0.05$ vs normal control, [b]$p < 0.05$ vs DMH control.

Please cite this article in press as: N.D. Reddy et al., *In vitro* and *in vivo* evaluation of novel cinnamyl sulfonamide hydroxamate derivative against colon adenocarcinoma, Chemico-Biological Interactions (2015), http://dx.doi.org/10.1016/j.cbi.2015.03.015

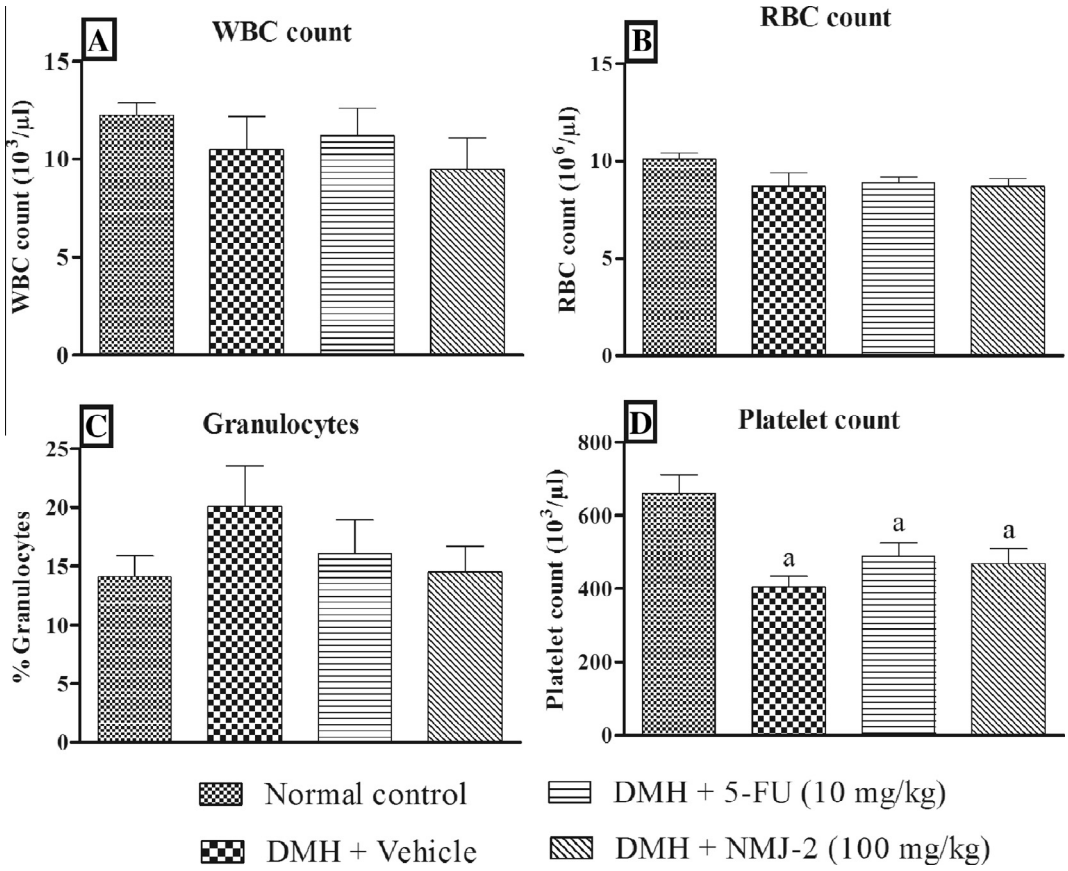

Fig. 9. Effect of DMH + 5-FU (10 mg/kg, *i.p.*) and DMH + NMJ-2 (100 mg/kg, *p.o.*) administration for 21 days on blood profile. (A) WBC count, (B) RBC count, (C) granulocytes count, (D) platelet count. All values are mean ± SEM of six samples. [a]$p < 0.05$ vs normal control, [b]$p < 0.05$ vs DMH control.

such as Apc, K-ras, β-catenin and thus leads to susceptibility of specific adenocarcinoma of colon [38–40]. The following parameters were monitored in this model.

3.9.1. ACF, adenocarcinoma incidence and count

Aberrant crypt foci (ACF) are well accepted biomarkers for the detection of colon cancer [41]. The ACF count helps in the analysis of the extent of damage to the mucosa of colon by DMH treatment. In this present study, DMH control showed 100% ACF incidence throughout treatment groups whereas, in normal control the incidence was 0%. Further, tissue sections from distal 5 cm^2 of colon tissues were selected and the ACFs in all the treatment groups such as DMH control, 5-FU and NMJ-2 were observed as 84.24 ± 7.6, 58.5 ± 1.0 and 64.5 ± 6.7, respectively. Besides, the number of ACFs were also significantly ($p < 0.05$) reduced (about ~30%) in both 5-FU and NMJ-2 treated groups as compared with that of DMH control. The colon adenocarcinoma was found in all the treatment groups. However, 5-FU and NMJ-2 treatment shown a 50% reduction in adenocarcinoma count when compared with that of DMH control as shown in Table 4. NMJ-2 showed comparable anti-cancer efficacy with the standard 5-FU.

3.9.2. Biochemical parameters

TNF-α and IL-6 are known markers of tissue inflammation. The metabolites of DMH formed in the liver are transported to colon via bile and blood to cause methylation of colonic DNA leading to oxidative stress and inflammation which eventually cause multiple mutations in genes [40]. The major pathway for NO metabolism is oxidation. This involves the step where NO is completely metabolized to nitrite and nitrate in the body [42]. The quantification of NO metabolites in biological samples provides valuable information about nitrosative and nitrative stress. In blood, plasma, other physiological fluids, tissue homogenates or buffers, metabolites of NO remain stable for several hours and can be estimated by different methods [43].

From our study, it was observed that DMH control had raised TNF-α, IL-6, nitrite and nitrate contents as compared to normal control as shown in Fig. 7. It was found that in DMH control there was a 20-fold increase in TNF-α level. However, the IL-6 level was increased by 10-fold when compared with that of normal control. Further, 5-FU and NMJ-2 treatment led to a significant ($p < 0.05$) decrease in the TNF-α, IL-6, nitrite and nitrate contents as compared to DMH control.

3.9.3. Organ index

A rise in the colon weight/length ratio indicates colonic edema or hyperplasia due to tissue injury or inflammation leading to development of micro adenomas, adenomas and adenocarcinomas [44]. In the present study, the rat colon weight/length ratio was significantly increased ($p < 0.05$) in DMH control as compared with normal control. However, in 5-FU and NMJ-2 treated groups, the ratio was reduced but statistically not significant when compared with DMH control (Fig. 8). No significant changes were observed in liver and spleen indices in any of the treatment groups when compared with normal and DMH controls.

3.9.4. Hematological parameters

None of the treatment groups had significant alterations in WBC, RBC and granulocyte count. However, the total WBC count was found to be slightly reduced in NMJ-2 treatment which was

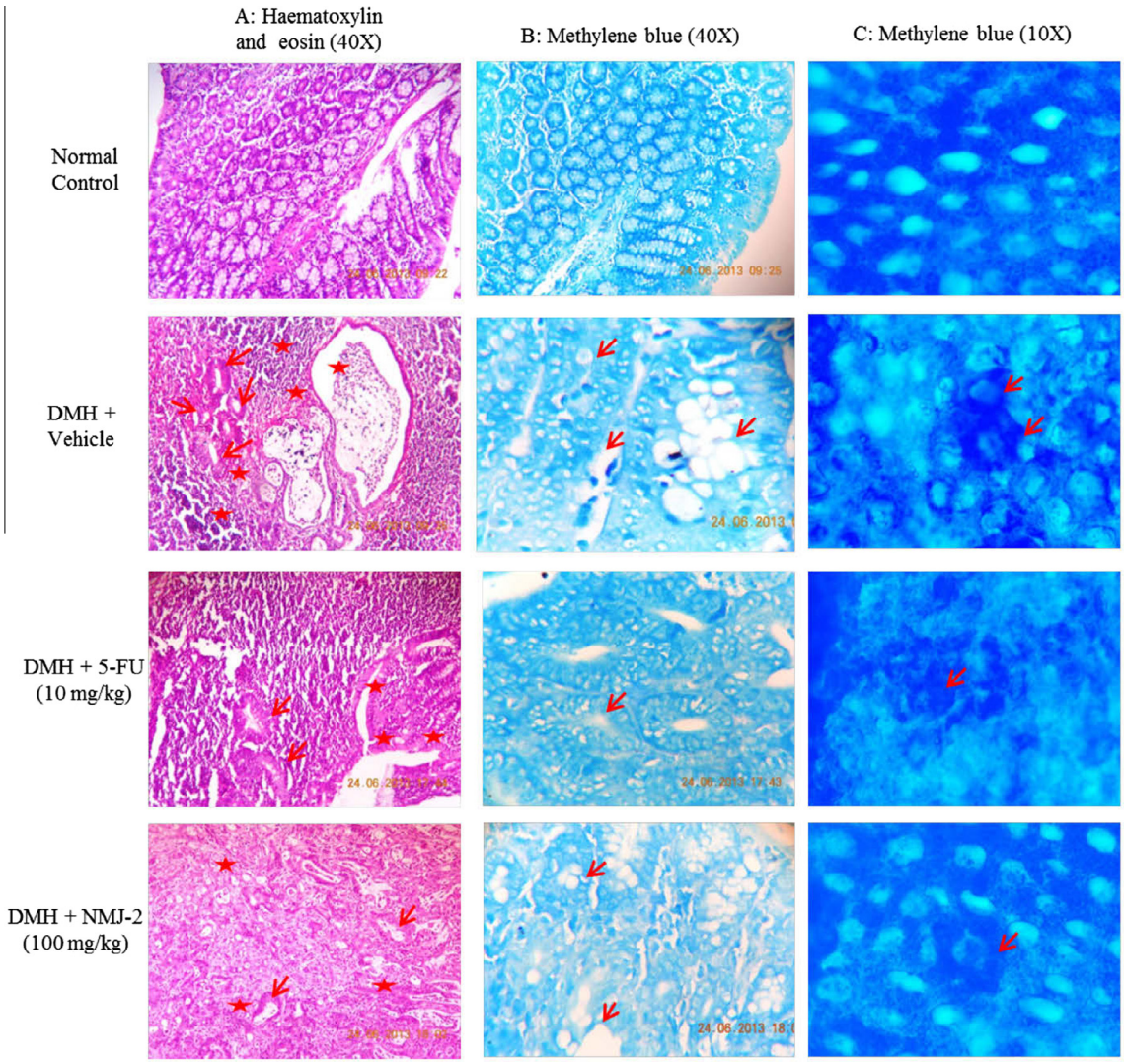

Fig. 10. Effect of DMH + 5-FU (10 mg/kg, *i.p.*) and DMH + NMJ-2 (100 mg/kg, *p.o.*) administration for 21 days on histopathology of colon. (A) Hematoxylin and eosin staining in 5 μm colonic section (40×); (B) methylene blue staining with 5 μm colonic section (40×); (C) methylene blue staining with formalin fixed 5 cm^2 intact colon tissue (10×). The inflammatory lesions were indicated by stars and ACFs were indicated by arrows in hematoxylin and eosin (H and E) stained sections.

statistically insignificant. A decrease in the granulocyte count was observed with 5-FU and NMJ-2 compared to DMH control which was statistically insignificant (Fig. 9). Further, it was observed that there was a significant ($p < 0.05$) decrease in platelet count of DMH control, 5-FU and NMJ-2 treatment compared to normal control.

3.9.5. Histopathology of colon

The colon tissue of normal control had the usual histoarchitecture with no signs of crypt abscess and dysplasia. However, in DMH control group, it was observed that the colonic mucosa had enlarged with crypt abscess, infiltration of inflammatory cells, aberrant crypt foci formation and nuclear enlargement with adenocarcinoma [40]. Hematoxylin–eosin and methylene blue stained ACFs are shown by arrows in Fig. 10. Absence of mucosal crypt abscess, reduced number of ACFs with putative pre-neoplastic lesions and minimal infiltration of inflammatory cells were the key features of 5-FU and NMJ-2 treatments.

4. Conclusion

Among the synthesized bio-isosters, NMJ-2, a thiophene derivative, was found to be the potent candidate for the treatment of colon cancer in both *in vitro* and *in vivo* models. Our research findings showed that NMJ-2 acts through HDAC inhibition and induction of intrinsic mitochondrial apoptotic pathway in colon cancer cells. *In vivo* studies on DMH-induced colon adenocarcinoma in rats showed a considerable reduction in ACFs and adenocarcinoma count, decreased inflammatory mediators (TNF-α, IL-6), normal hematological parameters, organ index, anatomical and histopathological characteristics of the colon. These results indicate NMJ-2 as a promising anti-cancer agent with efficacy at par with the existing standard 5-FU. The effect of the compound can be further assessed in suitable transgenic cancer models to mimic the human condition and to better understand its potential as a drug.

Conflict of Interest

The author(s) declare(s) that they have no conflicts of interest to disclose.

Transparency Document

The Transparency document associated with this article can be found in the online version.

Acknowledgements

The authors would like to acknowledge the Department of Pharmacology, Manipal College of Pharmaceutical Sciences, Manipal University, Manipal, Karnataka, India for providing the facilities to carry out the work. For purchase of biochemical kits and antibodies used in the study, the financial support was obtained from Department of Science & Technology – Science and Engineering Research Board (DST-SERB), New Delhi, India through Extra Mural Research Funding Scheme [Grant Sanction No.: SR/SO/HS-0282/2012]. The flow cytometer used in the study was obtained from All India Council for Technical Education through Research Promotion Scheme (AICTE-RPS) [Grant Sanction No.: 20/AICTE/RIFD/RPS/(POLICY-1)/64/2013-14] and Modernization and Removal of Obsolescences (MODROB) [Grant Sanction No.: 9-126/RIFD/MODROB/Policy-1/2013-14(Pvt.)].

References

[1] A. Jemal, F. Bray, M.M. Center, J. Ferlay, E. Ward, D. Forman, Global cancer statistics, CA-Cancer J. Clin. 61 (2011) 69–90.
[2] Globocan 2012, International Agency for Research on Cancer. Available at: http://globocan.iarc.fr/Pages/fact_sheets_cancer.aspx. Accessed on 1 August 2014.
[3] F. Bray, J.S. Ren, E. Masuyer, J. Ferlay, Global estimates of cancer prevalence for 27 sites in the adult population in 2008, Int. J. Cancer 132 (2013) 1133–1145.
[4] M.H. Myers, L.A.G. Ries, Cancer patient survival rates: Seer program results for 10 years of follow-up, CA-Cancer J. Clin. 39 (1989) 21–32.
[5] E.R. Fearon, B. Vogelstein, A genetic model for colorectal tumorigenesis, Cell 61 (1990) 759–767.
[6] M.F. Fraga, E. Ballestar, M.F. Paz, S. Ropero, F. Setien, M.L. Ballestar, D. Heine-Suner, J.C. Cigudosa, M. Urioste, J. Benitez, M. Boix-Chornet, A. Sanchez-Aguilera, C. Ling, E. Carlsson, P. Poulsen, A. Vaag, Z. Stephan, T.D. Spector, Y.-Z. Wu, C. Plass, M. Esteller, Epigenetic differences arise during the lifetime of monozygotic twins, Proc. Natl. Acad. Sci. U.S.A. 102 (2005) 10604–10609.
[7] H.J. Kim, S.C. Bae, Histone deacetylase inhibitors: molecular mechanisms of action and clinical trials as anti-cancer drugs, Am. J. Transl. Res. 3 (2011) 166–179.
[8] A. Taufel, A.Y. Leung, S. Foster, Encyclopedia of Common Natural Ingredients Used in Food, Drugs and Cosmetics, second ed., John Wiley & Sons Inc, New York, USA, 1996.
[9] P. De, M. Baltas, F. Bedos-Belval, Cinnamic acid derivatives as anticancer agents-a review, Curr. Med. Chem. 18 (2011) 1672–1703.
[10] T.L. Lemke, D.A. Williams, V.F. Roche, S.W. Zito, Foye's Principles of Medicinal Chemistry, seventh ed., Lippincott Williams & Wilkins, Philadelphia, USA, 2012.
[11] P.W. Finn, M. Bandara, C. Butcher, A. Finn, R. Hollinshead, N. Khan, N. Law, S. Murthy, R. Romero, C. Watkins, V. Andrianov, R.M. Bokaldere, K. Dikovska, V. Gailite, E. Loza, I. Piskunova, I. Starchenkov, M. Vorona, I. Kalvinsh, Novel sulfonamide derivatives as inhibitors of histone deacetylase, Helv. Chim. Acta 88 (2005) 1630–1657.
[12] X. Deng, N.S. Mani, A facile, environmentally benign sulfonamide synthesis in water, Green Chem. 8 (2006) 835–838.
[13] A.S. Reddy, M.S. Kumar, G.R. Reddy, A convenient method for the preparation of hydroxamic acids, Tetrahedron Lett. 41 (2000) 6285–6288.
[14] S. Talwar, H.V. Jagani, P.G. Nayak, N. Kumar, A. Kishore, P. Bansal, R.R. Shenoy, K. Nandakumar, Toxicological evaluation of *Terminalia paniculata* bark extract and its protective effect against CCl4-induced liver injury in rodents, BMC Complement Altern. Med. 13 (2013) 127.
[15] M. Fournel, C. Bonfils, Y. Hou, P.T. Yan, M.-C. Trachy-Bourget, A. Kalita, J. Liu, A.-H. Lu, N.Z. Zhou, M.-F. Robert, J. Gillespie, J.J. Wang, H.l.n. Ste-Croix, J. Rahil, S. Lefebvre, O. Moradei, D. Delorme, A.R. MacLeod, J.M. Besterman, Z. Li, MGCD0103, a novel isotype-selective histone deacetylase inhibitor, has broad spectrum antitumor activity in vitro and in vivo, Mol. Cancer Ther. 7 (2008) 759–768.
[16] P.G. Nayak, P. Paul, P. Bansal, N.G. Kutty, K.S.R. Pai, Sesamol prevents doxorubicin-induced oxidative damage and toxicity on H9c2 cardiomyoblasts, J. Pharm. Pharmacol. 65 1083–1093.
[17] A.M. Roy, M.S. Baliga, S.K. Katiyar, Epigallocatechin-3-gallate induces apoptosis in estrogen receptor-negative human breast carcinoma cells via modulation in protein expression of p53 and Bax and caspase-3 activation, Mol. Cancer Ther. 4 (2005) 81–90.
[18] P. Jain, N. Kumar, V.R. Josyula, H.V. Jagani, N. Udupa, C. Mallikarjuna Rao, P. Vasanth Raj, A study on the role of (+)-catechin in suppression of HepG2 proliferation via caspase dependent pathway and enhancement of its in vitro and in vivo cytotoxic potential through liposomal formulation, Eur. J. Pharm. Sci. 50 (2013) 353–365.
[19] G. Mathew, A. Jacob, E. Durgashivaprasad, N.D. Reddy, M.K. Unnikrishnan, 6b,11b-Dihydroxy-6b,11b-dihydro-7H-indeno[1,2-b]naphtho[2,1-d]furan-7-one (DHFO), a small molecule targeting NF-kappaB, demonstrates therapeutic potential in immunopathogenic chronic inflammatory conditions, Int. Immunopharmacol. 15 (2013) 182–189.
[20] F.E. Ghadi, A.R. Ghara, S. Bhattacharyya, D.K. Dhawan, Selenium as a chemopreventive agent in experimentally induced colon carcinogenesis, World J. Gastrointest. Oncol. 1 (2009) 74–81.
[21] A. Tsunoda, M. Shibusawa, Y. Tsunoda, N. Yokoyama, K. Nakao, M. Kusano, N. Nomura, S. Nagayama, T. Takechi, Antitumor effect of S-1 on DMH induced colon cancer in rats, Anticancer Res. 18 (1998) 1137–1141.
[22] Mudgal Jayesh, Mathew Geetha, G. Nayak Pawan, D. Reddy Nitin, Namdeo Neelesh, R. Kumar Ravilla, Kantamaneni Chaitanya, R. Chamallamudi Mallikarjuna, Remedial effects of novel 2,3-disubstituted thiazolidin-4-ones in chemical mediated inflammation, Chem. Biol. Interact. 210 (2014) 34–42.
[23] K.M. Miranda, M.G. Espey, D.A. Wink, A. Rapid, Simple spectrophotometric method for simultaneous detection of nitrate and nitrite, Nitric Oxide 5 (2001) 62–71.
[24] B. Schnetger, C. Lehners, Determination of nitrate plus nitrite in small volume marine water samples using vanadium(III)chloride as a reduction agent, Mar. Chem. 160 (2014) 91–98.
[25] C. Bonfils, A. Kalita, M. Dubay, L.L. Siu, M.A. Carducci, G. Reid, R.E. Martell, J.M. Besterman, Z. Li, Evaluation of the pharmacodynamic effects of MGCD0103 from preclinical models to human using a novel HDAC enzyme assay, Clin. Can. Res. 14 (2008) 3441–3449.
[26] N. Kumar, V.P. Raj, B.S. Jayshree, S.S. Kar, A. Anandam, S. Thomas, P. Jain, A. Rai, C.M. Rao, Elucidation of structure-activity relationship of 2-quinolone derivatives and exploration of their antitumor potential through Bax-induced apoptotic pathway, Chem. Biol. Drug Des. 80 (2012) 291–299.
[27] S. Temple, M.C. Raff, Clonal analysis of oligodendrocyte development in culture: evidence for a developmental clock that counts cell divisions, Cell 44 (1986) 773–779.
[28] S.J. Elledge, Cell cycle checkpoints: preventing an identity crisis, Science 274 (1996) 1664–1672.
[29] B. Verhoven, R.A. Schlegel, P. Williamson, Mechanisms of phosphatidylserine exposure, a phagocyte recognition signal, on apoptotic T lymphocytes, J. Exp. Med. 182 (1995) 1597–1601.
[30] J.G. Walsh, S.P. Cullen, C. Sheridan, A.U. Luthi, C. Gerner, S.J. Martin, Executioner caspase-3 and caspase-7 are functionally distinct proteases, Proc. Natl. Acad. Sci. U.S.A. 105 (2008) 12815–12819.
[31] H.J. Brady, G. Gil-Gomez, Bax. The pro-apoptotic Bcl-2 family member, Bax, Int. J. Biochem. Cell Biol. 30 (1998) 647–650.
[32] S. Shimizu, M. Narita, Y. Tsujimoto, Bcl-2 family proteins regulate the release of apoptogenic cytochrome c by the mitochondrial channel VDAC, Nature 399 (1999) 483–487.
[33] M. Hanada, C. Aime-Sempe, T. Sato, J.C. Reed, Structure-function analysis of Bcl-2 protein. Identification of conserved domains important for homodimerization with Bcl-2 and heterodimerization with Bax, J. Biol. Chem. 270 (1995) 11962–11969.
[34] Y. Shi, J. Chen, C. Weng, R. Chen, Y. Zheng, Q. Chen, H. Tang, Identification of the protein-protein contact site and interaction mode of human VDAC1 with Bcl-2 family proteins, Biochem. Biophys. Res. Commun. 305 (2003) 989–996.
[35] C. Weng, Y. Li, D. Xu, Y. Shi, H. Tang, Specific cleavage of Mcl-1 by caspase-3 in tumor necrosis factor-related apoptosis-inducing ligand (TRAIL)-induced apoptosis in jurkat leukemia T cells, J. Biol. Chem. 280 (2005) 10491–10500.
[36] P.C. Nowell, C.M. Choce, Chromosomes, genes, and cancer, Am. J. Pathol. 125 (1986) 7–15.
[37] D. Hanahan, R.A. Weinberg, The hallmarks of cancer, Cell (2000) 57–70.
[38] J.A. Swenberg, H.K. Cooper, J. Bucheler, P. Kleihues, 1,2-Dimethylhydrazine-induced methylation of DNA bases in various rat organs and the effect of pretreatment with disulfiram, Cancer Res. 39 (1979) 465–467.
[39] L.C. Boffa, R.J. Gruss, V.G. Allfrey, Aberrant and nonrandom methylation of chromosomal DNA-binding proteins of colonic epithelial cells by 1,2-dimethylhydrazine, Cancer Res. 42 (1982) 382–388.
[40] O.O. Hamiza, M.U. Rehman, M. Tahir, R. Khan, A.Q. Khan, A. Lateef, F. Ali, S. Sultana, Amelioration of 1,2 dimethylhydrazine (DMH) induced colon oxidative stress, inflammation and tumor promotion response by tannic acid in Wistar rats, Asian Pac. J. Cancer Prev. 13 (2012) 4393–4402.
[41] T. Tanaka, Colorectal carcinogenesis: review of human and experimental animal studies, J. Carcinog. 8 (2009). 5–5.
[42] K. Yoshida, K. Kasama, M. Kitabatake, M. Imai, Biotransformation of nitric oxide, nitrite and nitrate, Int. Arch. Occup. Environ. Health 52 (1983) 103–115.
[43] N.S. Bryan, M.B. Grisham, Methods to detect nitric oxide and its metabolites in biological samples, Free Radical Biol. Med. 43 (2007) 645–657.
[44] O. Morteau, S.G. Morham, R. Sellon, L.A. Dieleman, R. Langenbach, O. Smithies, R.B. Sartor, Impaired mucosal defense to acute colonic injury in mice lacking cyclooxygenase-1 or cyclooxygenase-2, J. Clin. Invest. 105 (2000) 469–478.